AFRL-RW-EG-TR-2011-032

TEXTURE EVOLUTION DURING DYNAMIC LOADING OF ECAP TANTALUM

Joel House
Philip Flater
Richard Harris
Robert De Angelis

AIR FORCE RESEARCH LABORATORY
MUNITIONS DIRECTORATE
101 W EGLIN BLVD
EGLIN AFB, FL 32542-6810

UNIVERSITY OF FLORIDA/REEF
1350 NORTH POQUITO ROAD
SHALIMAR, FL 32579

MAR 2011
INTERIM REPORT

DISTRIBUTION A. Approved for public release, distribution unlimited. 96th ABW/PA Approval and Clearance # 96ABW-2011-0174, dated 05 April 2011.

AIR FORCE RESEARCH LABORATORY
MUNITIONS DIRECTORATE

■ **Air Force Materiel Command** ■ **United States Air Force** ■ **Eglin Air Force Base, FL 32542**

REPORT DOCUMENTATION PAGE

Form Approved
OMB No. 0704-0188

1. REPORT DATE
10-MAR-2011

2. REPORT TYPE
INTERIM

3. DATES COVERED *(From - To)*
MAR, 2008-DEC, 2010

4. TITLE AND SUBTITLE
TEXTURE EVOLUTION DURING DYNAMIC LOADING OF ECAP TANTALUM

5a. CONTRACT NUMBER

5b. GRANT NUMBER

5c. PROGRAM ELEMENT NUMBER
62602F

6. AUTHOR(S)
Joel House, Philip Flater, Richard Harris, Robert De Angelis

5d. PROJECT NUMBER
2502

5e. TASK NUMBER
12

5f. WORK UNIT NUMBER
28

7. PERFORMING ORGANIZATION NAME(S) AND ADDRESS(ES)

Air Force Research Laboratory
AFRL/RWMWD
101 W Eglin Blvd.
Eglin AFB, FL 32542-6810

U. of Florida/REEF
1350 N. Poquito Rd.
Shalimar, FL 32579

8. PERFORMING ORGANIZATION REPORT NUMBER

AFRL-RW-EG-TR-2011-032

9. SPONSORING / MONITORING AGENCY NAME(S) AND ADDRESS(ES)
Air Force Research Laboratory, Munitions Directorate
AFRL/RWMWD
101 West Eglin Boulevard
Eglin AFB, FL 32542-6810

10. SPONSOR/MONITOR'S ACRONYM(S)
AFRL-RW-EG

11. SPONSOR/MONITOR'S REPORT NUMBER(S)
AFRL-RW-EG-TR-2011-032

12. DISTRIBUTION / AVAILABILITY STATEMENT

Approved for public release, distribution unlimited. 96th ABW/PA Approval and Clearance #96ABW-2011-0174, dated 05 April 2011.

13. SUPPLEMENTARY NOTES
DISTRIBUTION STATEMENT INDICATING AUTHORIZED ACCESS IS ON THE COVER PAGE AND BLOCK 12 OF THIS FORM.
DATA RIGHTS RESTRICTIONS AND AVAILABILITY OF THIS REPORT ARE SHOWN ON THE NOTICE AND SIGNATURE PAGE.

14. ABSTRACT

A Taylor Impact experiment was conducted on commercially pure Ta subjected to thermo-mechanical processing that included Equal Channel Angular Pressing (ECAP), forging and annealing. The recovered specimen profile geometry was measured to characterize the extent of plastic anisotropy. Electron Backscattered Diffraction (EBSD) was used to characterize the texture evolution under dynamic loading. The as forged and annealed texture consisted of (111)[1-21] and (111)[-1-12] texture components. A series of EBSD crystal direction maps along the axial length of the specimen revealed that the texture evolution was described by a 19.5° rotation about the [-110] and [10-1] axes. This rotation was sufficient to bring {111} texture components of the original disk into alignment with the compression axis of the Taylor Impact specimen.

15. SUBJECT TERMS
TANTALUM, EQUAL CHANNEL ANGULAR PRESSING, ECAP, TAYLOR IMPACT, TEXTURE,

16. SECURITY CLASSIFICATION OF:			17. LIMITATION OF ABSTRACT	18. NUMBER OF PAGES	19a. NAME OF RESPONSIBLE PERSON
					Joel House
a. REPORT	b. ABSTRACT	c. THIS PAGE	UL	15	19b. TELEPHONE NUMBER *(include area code)*
UNCLASSIFIED	UNCLASSIFIED	UNCLASSIFIED			850-882-7987

Standard Form 298 (Rev. 8-98)
Prescribed by ANSI Std. Z39.18

NOTICE AND SIGNATURE PAGE

AFRL-RW-EG-TR-2011-032 HAS BEEN REVIEWED AND IS APPROVED FOR PUBLICATION IN ACCORDANCE WITH ASSIGNED DISTRIBUTION STATEMENT.

FOR THE DIRECTOR:

/signed/	/signed/	/signed/
HOWARD G. WHITE	MATTHEW J. MATYAC	JOEL W. HOUSE
Technical Advisor	Technical Advisor	Program Manager
Ordnance Division	Damage Mechanisms Branch	Damage Mechanisms Branch

Table of Contents

Executive Summary …………………………………………………… 1

1.0 Introduction ………………………………………………………2

2.0 Material …………………………………………………………..2

3.0 Experiment ………………………………………………………3

4.0 Results ……………………………………………………………4

5.0 Discussion ……………………………………………………..7

6.0 Conclusions …………………………………………………....9

Acknowledgements ……………………………………………….10

References ……………………………………………………….....10

Executive Summary

A new Environmental Scanning Electron Microscope (ESEM) was installed at the Advance Warhead Experimentation Facility (AWEF) in March of 2008. This ESEM provided the Damage Mechanisms Branch of the Ordnance Division a tool for characterizing the response of deformed materials. From October 2007 until February 2009 personnel from the Damage Mechanisms Branch of the Air Force Research Laboratory have been active in the installation of the unit, and the initial training phase of its operation and maintenance. One of the principle technologies associated with the ESEM unit is the use of electron backscattered diffraction (EBSD) to create crystal direction maps. These maps provided spatially resolved data on grain orientation within a metal sample.

This report describes 1) the thermo-mechanical processing of ECAP tantalum, 2) a brief description of a Taylor Impact experiment using ECAP tantalum, and 3) data gathered from a recovered specimen. Using the ESEM, a recovered specimen was interrogated to determine a series of crystal direction maps through the deformation zone at 0.15, 0.44, 0.75, 1.25, 2.27, 2.5, 5, 10, 15 and 19 mm from the impact interface. All of the measurements were made along the center-line of the sample. Using the sequence of crystal direction maps, the mechanics of grain rotation as plastic strain was accumulated in the tantalum sample was determined. This data and the subsequent analysis provided insight to the deformation mechanisms resulting from high strain rate loading of tantalum.

The information generated in this report provided data to improve the understanding of the behavior of materials loaded dynamically. This information will be used to improve thermo-mechanical processing for optimizing the properties of tantalum and to validate the accuracy of simulation tools that calculate texture evolution in metals. This insight provides the Air Force with the ability to improve processing, repeatability, performance and to reduce cost of metal components.

1.0 Introduction

Mechanical and physical properties of commercially pure tantalum make it an ideal material for high strain rate applications, such as munitions.[1-5] These high strain rate applications require properties of high density, and good formability. Mechanical properties like flow strength, work hardening rate, strain rate and temperature sensitivity, etc. must be sufficiently well characterized and controlled such that optimum and repeatable performance can be achieved.[6-9]

Since the introduction of the Taylor model, the relationships between deformation mechanisms and texture development has been an active area of research. [10] Generally these investigations have considered the roles of deformation mechanisms, deformation geometry, active slip systems, twinning, and thermo-mechanical history on the formation of texture. For compressive loading of tantalum, the texture have been observed to consist of a strong (ND)$\|$(111) and a weak (ND)$\|$(001). The objective of this investigation was to develop an understanding of the role of plastic deformation on the formation of texture, specifically, the texture evolution that occurs during high strain rate loading of tantalum. Dynamic loading was achieved using the Taylor Impact experiment.[11]

In this study, large diameter commercially pure tantalum rod stock was processed by ECAP, followed by forging.[12-14] The ECAP introduced simple shear deformation into the structure for grain refinement, while the forging formed sections of the rod into large diameter disks. Taylor Impact specimens fabricated from the disk were tested to investigate the influence of thermo-mechanical history on texture evolution and plastic anisotropy during high rate loading.[15-17]

2.0 Material

The commercially pure tantalums used in this investigation were obtained from Cabot Performance Metals and H.C. Starck Inc. The starting rod geometry from the mill was 63 mm (2.50 inch) diameter. Segments of the original rod where processed by ECAP eight times through tooling with a 135˚ included angle between the entrance and exit channels. After each pass, the ingot was rotated 180˚, route B. The ECAP processing generated a strain of 0.5 per pass.[18] After ECAP the rod segments were forged to 6.3 mm (0.25 inch) thick disks. The engineering strain introduced by forging was greater than 90%. Taylor Impact specimens were fabricated with the longitudinal axes of the specimens aligned in the radial direction of the forged disks. The geometry of the Taylor specimens was 5.3 mm (0.209 inch) diameter by 53.3 mm (2.10 inch) length.

Specimens of Cabot tantalum were annealed one hour in a vacuum furnace at 950˚C and 1250˚C to produce fine and coarse grain microstructures. Starck tantalum specimens were vacuum annealed one hour at temperatures of 1050˚C and 1250˚C to produce fine and coarse grain microstructures. All specimens were furnace cooled from the annealing temperatures.

3.0 Experiment

The Taylor Impact experiment consists of launching a plane-ended cylindrical specimen against a rigid target. The launch tube used in this study had a 5.33 mm (0.210 inch) bore diameter. The impact surface was a highly polished 4340 steel anvil, heat treated to Rc hardness of 58. Two independent measurement techniques were used to determine the projectile impact velocity. One system used a pair of pressure gauges, the other used a pair of lasers. The range of projectile impact velocities were from 157 m/s to 205 m/s. The final geometries of the recovered impact specimens were measured using an optical comparator. To analyze the deformed microstructures, the samples were sectioned and prepared using standard grinding and polishing techniques for tantalum.[19] The structures of the deformed samples interrogated using a FEI Quanta 200, field emission gun scanning electron microscope (SEM), equipped with EBSD hardware and software provided by EDAX/TSL.

4.0 Results

After impact, the circular cross-section of the impact specimens was plastically deformed into an ellipsoidal geometry. The major axis of the ellipse was aligned with the in-plane direction of the forged disk, and the minor axis with the normal direction (ND). This plastic anisotropy was characterized by measuring the specimen profile diameter in both the major (aligned with the in-plane direction) and minor (aligned with the ND direction) planes using an optical comparator. A data set for coarse grain Cabot tantalum is shown in Fig. 1a. Using the approximate analysis for engineering strain provided by Taylor in Reference 13, the compressive strains (negative) can be calculated from the profile diameters and the results are plotted as a function of axial position in Fig. 1b.

The recovered Taylor Impact specimens were sectioned parallel to the major profile plane (as shown in Fig. 1a). An EBSD crystal direction map collected on the Cabot coarse grain specimen 19 mm from the impact face on the longitudinal axis is shown in Fig. 2e. The strain introduced into the specimen at this position is zero, see Fig. 1a. The orientation distribution of the grains in Fig. 2e are shown in the (111) pole figure shown in Fig. 2b.

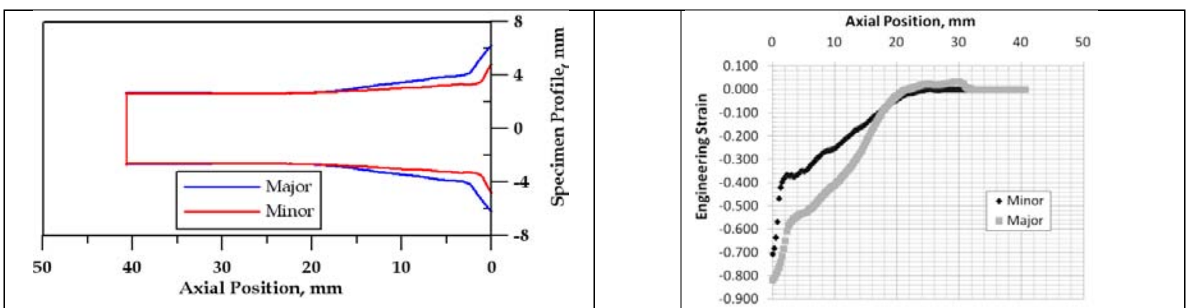

(a) (b)

Fig.1. Profile analysis of the recovered Taylor Impact specimen fabricated from the annealed Cabot tantalum, a) major and minor profile diameters, and b) engineering strain.

All pole figure were generated using 24th order spherical harmonics. The six fold symmetry of the (111) pole figure in Fig. 2b suggests that the annealed Cabot texture is comprised of two (111) components that are related by a 60˚ rotation. These texture components were determined using 30º deviations partitions about (111)[1-21],(shown in Figs. 2a and 2d), and the (111)[-1-12],(shown in Figs. 2c and 2f). The texture strengths of the partitioned components are stronger because data from the reduced areas shown in Figs. 2d, and 2f were employed in the normalization calculation needed to calculate times random numbers.

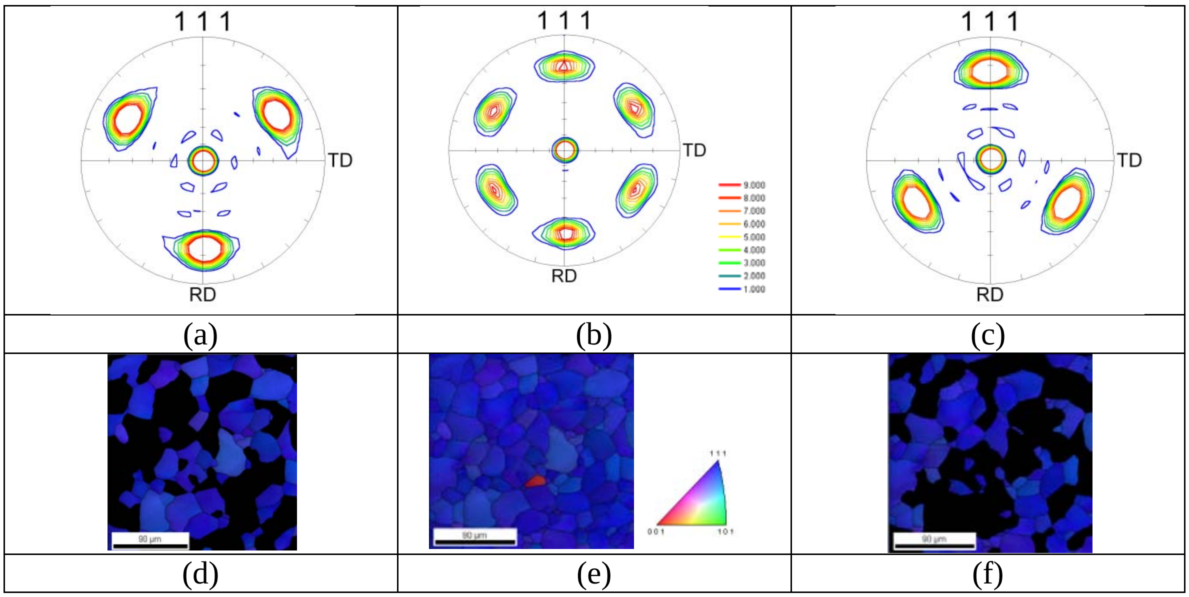

Fig.2. (111) pole figures and crystal direction maps of annealed Cabot Tantalum at 19 mm from the impact face, a) and d) data only from material within 30˚ of the (111)[1-21] orientation, b) and e) data from all of the material, c) and f) data only from material within 30˚ of the (111)[-1-12] orientation. The pole figures and crystal direction maps are viewed parallel to ND.

The direction labeled TD lies in the plane of the disk parallel to [-101] in the texture component (111)[1-21] and TD is parallel to [-110] for the (111)[-1-12] component. As will be discussed below these <110> directions are the rotation axes active in the evolution of the texture observed in the deformed portion of the Taylor Impact specimen.

The texture evolution in the plastically deformed region of the specimen was determined by recording a series of crystal direction maps at distances of 0.15, 0.44, 0.75, 1.25 2.27,2.5, 5, 10, 15 and 19 mm from the impact face along the specimen axis. These data sets were rotated 90º into the axial direction of the specimens, i.e., the Taylor impact specimen compression axes. Crystal direction maps and related (111) pole figures for the complete data set and the data contained in the 30 ºdeviation partitions (111)[1-21], and (111)[-1-12] are shown in Fig. 3.These data are reported in Fig. 3 were obtained at distances of 0.15, 5 and 19 mm from the impact face. The pole figures of the orientation

partitions in Fig. 3 show the opposite rotations of the two partitions. Rotations of 19.5 º about the <011> axes transforms a {111}<112> texture to a {112}<111> and visa versa. Here the (111)[1-21] partition rotates counterclockwise about the [-101] while the (111)[-1-12] partition rotates clockwise about the [-110]. These two rotations of 19.5 º change the texture from {112}<111> 19 mm from the impact face to {111}<112> 0.15 mm from the impact face.

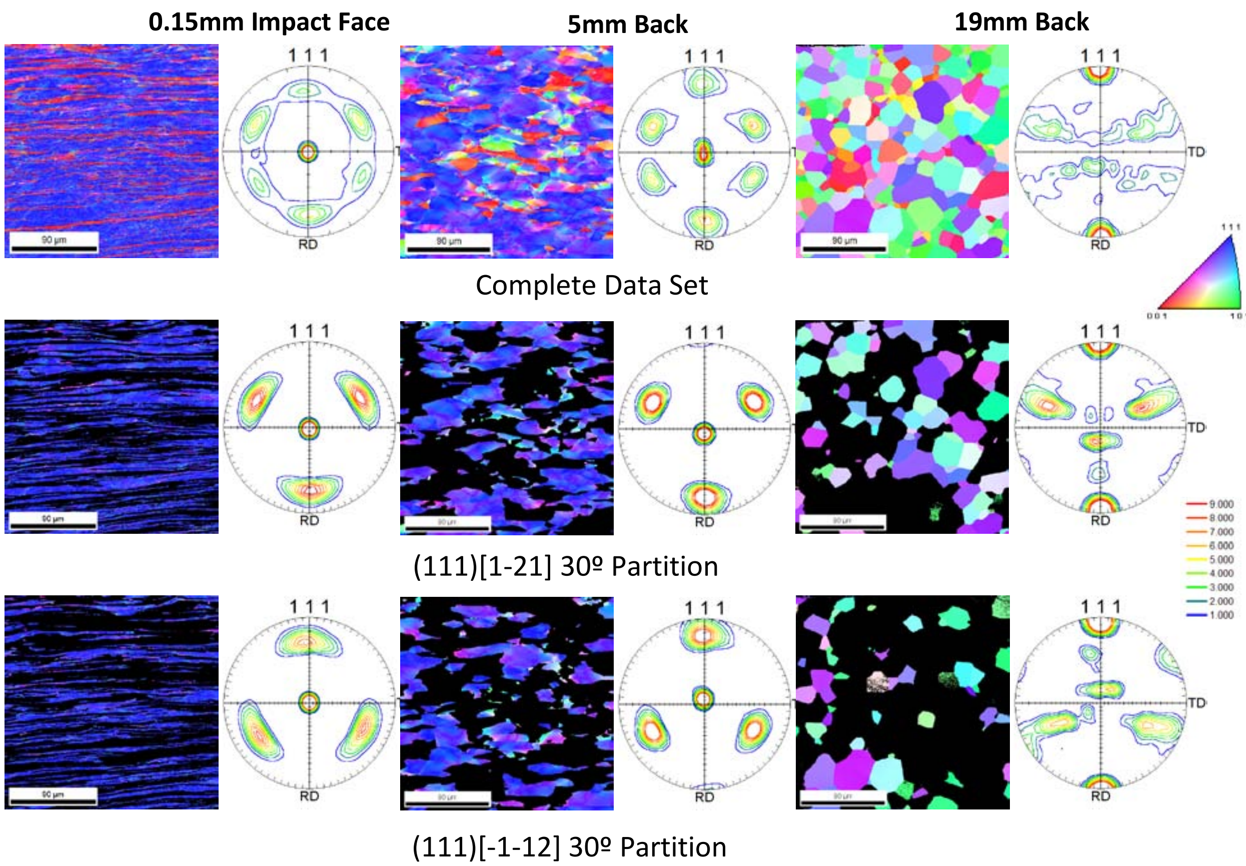

Fig. 3 Fine Grain Starck Axial View, Complete Data Set and Two (111) 30º Partitions

Rotations about the <110> as a function of axial position for fine and coarse grain Cabot and Starck tantalum are given in Table I along with the average values of the engineering strains. The rotations reported in Table I are the average of the rotations from the pole figures of the two {111}<112> partitions at each axial position. The orientations present at 0.15 mm from the impact face are 85% (111) and 15% (001). Similar splits in these orientations were observed on the impact face of tantalum Taylor impact specimens by Bingert et al. in Reference 17.

As reported by Boas and Schmid;[20] if {110} planes are the only active slip planes a [111] texture develops during compression of BCC metals. If {112} or {123} slip planes are active in addition to the {110} a [111] + [001] duplex texture forms. [111] + [001] duplex textures were observed 0.15 mm from the impact face of the Taylor specimens.

The analysis of the strains from profile dimensions of the Taylor Impact specimen is only an approximation for the true strain. This approximation is reasonable accurate in the deformation region beyond the mushroom diameter, roughly beginning at 5 mm from the impact face and extending further down the axis of the rod. In the region between the impact face and the 5 mm position the plastic strain varies significantly both in the axial and radial directions. The analysis of the profile diameter by Taylor to approximate strains did not make allowances for anisotropic material response.

Table I. Engineering Strains and Rotations Angles From {112}<111> for Taylor Impact Specimens

Axial Position, mm	Engineering Strain	Fine Grain Starck Degrees	Fine Grain Cabot Degrees	Coarse Grain Starck Degrees	Coarse Grain Cabot Degrees
19	0.00	19.5	19.5	19.5	19.5
15	0.18	16.3	15.5	12.5	17
10	0.25	9.4	9.5	8.5	10
5	0.34	5.9	5.9	7	6.9
2.5	0.36	4.5	6	7	5.8
2.27	0.38	6	6.5	7.5	5.5
1.25	0.4	5.9	4.5	7	8
0.75	0.54	4.7	3	6.8	6.1
0.44	0.64	2.7	1.6	4.2	4
0.15	0.8	1.2	0.5	1.3	0.9

The data in Table I are shown graphically in Fig. 4. Notice how the rotation angles demonstrate different behavior in the region 19 to 2.5 mm from the impact face compared to positions closer than 2.5 mm from the impact face. These changes in behavior of the rotation data correspond to changes in the deformation characteristics. As seen in Fig. 1b the region of inhomogeneous deformation of the specimen extends 2.5 mm in from the impact face. The strains experienced in the material closer than 2.5 mm from the impact face are of a different character and greater in magnitude. These account for the transition in the rotational behavior of the texture at positions less than 2.5 mm from the impact face.

These rotation data agree with the rotations observed by Barrett as a result of compression of a crystal of BCC iron. [21] He observed crystallographic a rotation of eight degrees toward the <111> at a compression of 27% and a rotation of twenty degrees toward the <111> at a 61% compression. The initial loading direction in Barrett’s investigation was near the center of the stereographic triangle.

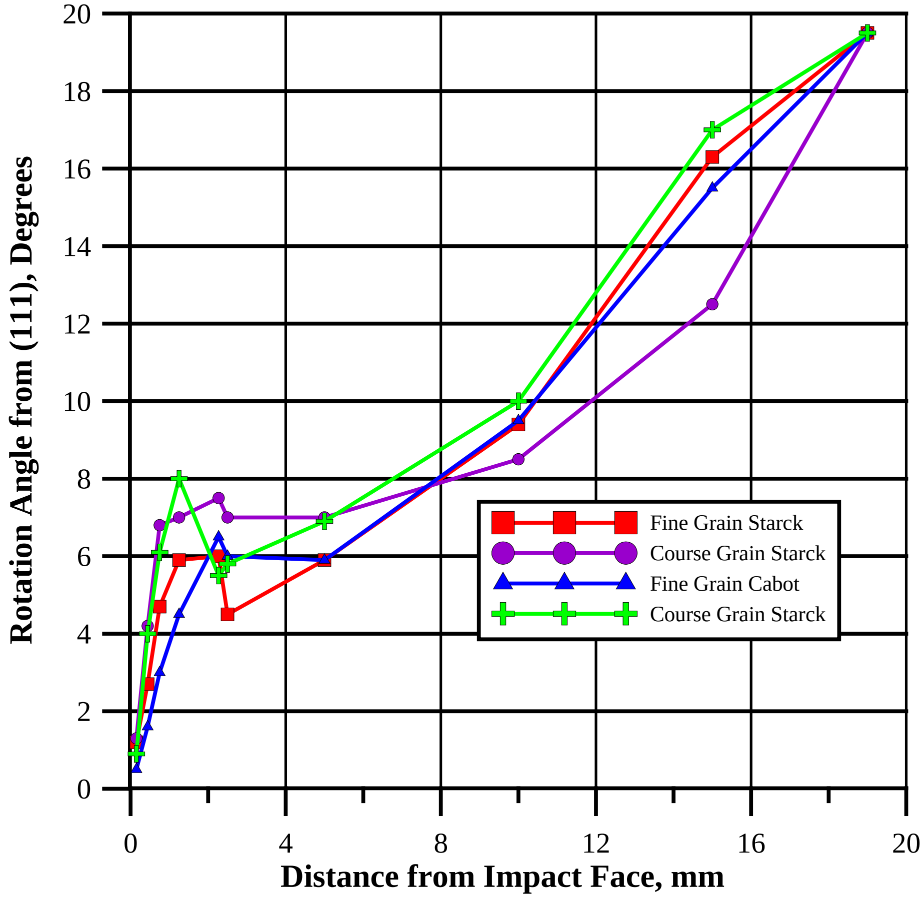

Fig. 4 Rotation Angles from {112}<111> as a Function of Distance from the Impact Face.

5.0 Discussion

The main point to be discussed is a probable explanation for the rotations observed in Fig. 4. This explanation can be arrived at through an analysis of the crystallography of BCC single crystal compression.

The texture at the impact interface consists of two superimposed textures (-1-11)[112] and (1-11)[121] and at 19 mm the texture components are (-1-12)[111] and (1-21)[111]. The duplex texture at the impact face is related to the duplex texture in the forged plate (textures at 19 mm) by 19.5º rotation about the [-110] and [-101] axis. The geometry of these texture relationships is shown in Figs. 5a and 5b.

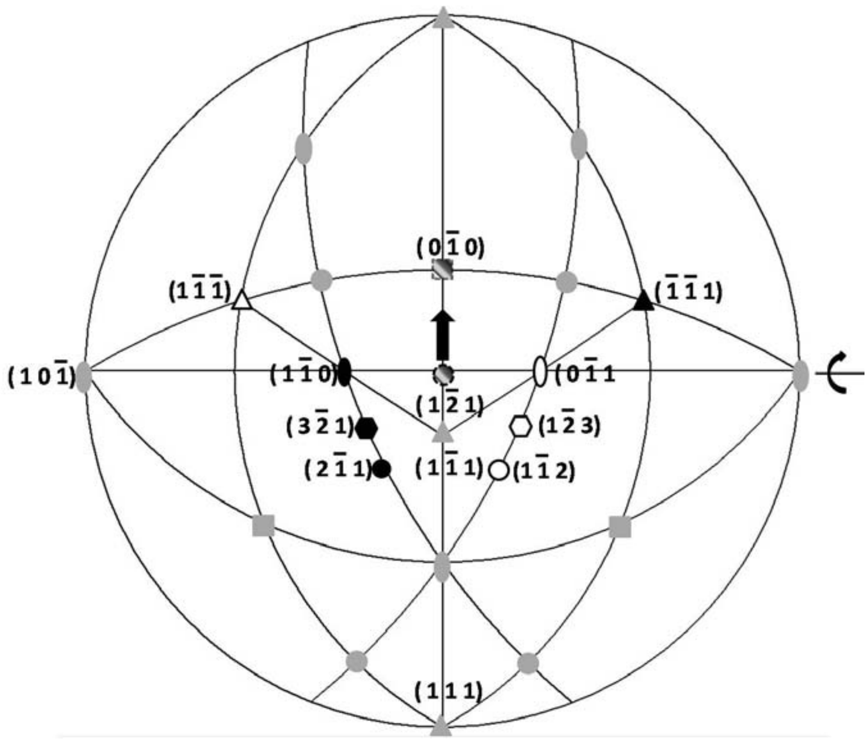

Fig. 5a (1-2 1) [111] pole figure showing (1-1-1) slip systems in open sympols and (-1-11) slip systems in solid symbols. Rotation of 19.5° about [10-1] changes the center of pole figure from(1-21) to (1-11).

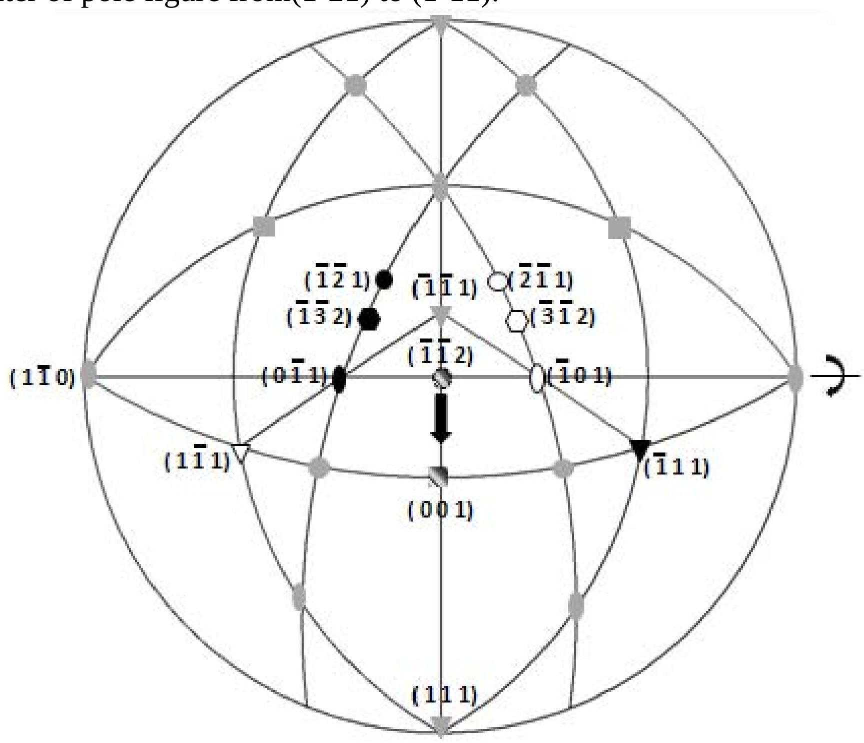

Fig. 5b (-1-1 2) [111] pole figure showing (1-1 1) slip systems in open sympols and (-1 1 1) slip systems in solid symbols. Rotation of 19.5° about [1-10] changes the center of pole figure from(-1-12) to (-1-11).

The slip systems available in the (1-21) [111] and (-1-12) [111] with the largest Schmid factors are shown in Table II. The pole figures containing the favored slip systems for these orientations are shown in Figs 5a and b. The active slip directions for the [1-21] loading axis in the (1-21) [111] texture are [1-1-1] and [-1-11]. Assuming these directions operate simultaneously and equally on loading the resulting motion of the crystal would be in the [0-10] direction as indicated in Fig. 5a. This motion rotates the [1-11] into the center of the pole figure. With sufficient deformation the [1-11] becomes aligned with the impact direction which is a stable position. For the (-1-12) [111] partition, the active slip directions are [1-11] and [-111] which when operating rotate the crystal toward the [001]. This motion will rotate the [-1-11] into the impact direction where it becomes a stable orientation (see Fig. 5b).

The rotation of the (1-11) to the center of the pole figure is accomplished by clockwise rotation about the [-101] (Fig.5a) while the (-1-11) rotates to the center of the pole figure by counter clockwise rotation about the [-110] (Fig. 5b).

Table II. Schmid Factors for Most Favorable Slip Systems for <112> Loading Axes

	$[1\,\bar{2}\,1]$ Axis		$[\bar{1}\,\bar{1}\,2]$ Axis	
Schmid Factor	Slip Plane	Slip Direction	Slip Plane	Slip Direction
0.411	$(1\,\bar{2}\,3)$	$[1\,\bar{1}\,\bar{1}]$	$(\bar{3}\,\bar{1}\,2)$	$[1\,\bar{1}\,1]$
	$(3\,\bar{2}\,1)$	$[\bar{1}\,\bar{1}\,1]$	$(\bar{1}\,\bar{3}\,2)$	$[\bar{1}\,1\,1]$
0.408	$(0\,\bar{1}\,1)$	$[1\,\bar{1}\,\bar{1}]$	$(\bar{1}\,0\,1)$	$[1\,\bar{1}\,1]$
	$(1\,\bar{1}\,0)$	$[\bar{1}\,\bar{1}\,1]$	$(0\,\bar{1}\,1)$	$[\bar{1}\,1\,1]$
0.393	$(1\,\bar{1}\,2)$	$[1\,\bar{1}\,\bar{1}]$	$(\bar{2}\,\bar{1}\,1)$	$[1\,\bar{1}\,1]$
	$(\bar{2}\,1\,\bar{1})$	$[\bar{1}\,\bar{1}\,1]$	$(\bar{1}\,\bar{2}\,1)$	$[\bar{1}\,1\,1]$

Conclusion

EBSD inspection of Taylor Impact specimens provides an excellent method to establish the dependence of texture variations on dynamic strain.

ECAP, forged and annealed tantalum plates have a two component texture consisting of (111)[1-21] and (111)[-1-12]. These textures produce loading directions of [1-21] and [-1-12] in Taylor Impact specimens cut in radial directions in the plate.

During loading the [1-21] and [-1-12] rotate 19.5º about the [10-1] and [1-10] respectively to produce a duplex (1-11) and (-1-11) texture.

Tantalum annealed in fine and coarse grain conditions have similar texture dependence on the dynamic strain created in the Taylor Impact experiment.

Acknowledgement

The authors thank Drs. Jim O'Brien and William Hosford for the ECAP processed tantalum. Discussions with John Bingert of Los Alamos National Laboratory are gratefully acknowledged.

References

[1] L.E. Murr, H. K. Shih and C-S Niou, Materials Characterization, 33 (1994) pp. 65-74.
[2] F. Cao, E.K. Cerreta, C.P. Trujillo and G.T. Gray III, Acta Materialia 56 (2008) pp. 5804-5817.
[3] E.C. Faccini, *Tantalum*, E.Chen, A. Crowson, E.Lavernia, W. Ebihara, P. Kumar (Eds.), TMS, Warrendale, PA (1996) pp. 73-94.
[4] H.K. Shin, L.E. Murr, C-S Niou, and L. Zernow, Scripta Met. et Mat. 29 (10) (1995) pp. 1291-1296.
[5] L. E. Murr, C-S Niou, J. C. Sanchez, and L. Zernow, Scripta Met. et Mat. 32(1) (1995) pp. 31-36.
[6] S. R. Chen and G. T. Gray III, Met. Trans. A, 27 A (10) (1996) pp. 2994-3006
[7] K. G. Hoge and A.K. Mukherjee, J. Mater. Sci. 12 (1977) pp. 1666-1672.
[8] C. A. Michaluk, *Tantalum*, E.Chen, A. Crowson, E.Lavernia, W. Ebihara, P. Kumar (Eds.), TMS, Warrendale, PA (1996) pp. 205-217.
[9] S. Nemat-Nasser and J.B. Isaacs, Acta Materialia 45 (3) (1997) pp.907-919.
[10] G.I. Taylor, J. Inst. of Metals, 62 (1938) pp. 307-324.
[11] G. I. Taylor, Proc. R. Soc of London, A 194, (1948) pp. 289-299.
[12] V. M. Segal, J. Mater. Sci. A197 (1995) pp. 157-164.
[13] S. N. Mathaudhu and K. T. Hartwig, Materials Science and Engineering A, 426 (2006) pp. 128-142.
[14] J. M. O'Brien and W. F. Hosford, AFRL-MN-EG-TR-2007-7000, Technical Report, Eglin AFB, FL, November 2006, Contract No. F08651-02-C-0023.
[15] P. J. Maudlin, J. F. Bingert, and G. T. Gray III, Int. J. of Plasticity 19 (2003) pp. 483-515.
[16] J. W. House and P. P. Gillis, Mat. Sci. Forum, vol. 408-412, (I) (2002) pp. 547-552.
[17] J.F. Bingert, T. A. Mason, G. C. Kashner, P. J. Maudlin and G. T. Gray III, *Electron Backscattered Diffraction in Materials Science*, A. J. Schwartz, M. Kumar, and B. Adams (Eds.), Plenum Publisher, New York, 2000, pp. 213-229.
[18] P. B. Berbon and T. G. Langdon, *Ultrafine Grained Materials*, R.S. Mishra, S. L. Semiatin, C. Suryanarayana, N. N. Thadhani (Eds.), The Minerals, Metals & Materials Society, 2000, pp. 381-392.
[19] A. M. Kelly, S. R. Bingert, and D. J. Thoma, Materials Characterization 32 (1) (1994) pp. 35-39.
[20] Boas and E. Schmid, Z. tech. Physik, 12,(1931) p71.

DISTRIBUTION LIST
AFRL-RW-EG-TR-2011-032

Defense Technical Information Center Attn: Acquisition (OCA) 8725 John J. Kingman Road, Ste 0944 Ft Belvoir, VA 22060-6218	1 Electronic Copy (1 File & 1 Format)

EGLIN AFB OFFICES:

AFRL/RWOC (STINFO Office)	- 1 Hard (Color) Copy
AFRL/RW CA-N	- STINFO Officer Provides Notice of Publication
AFRL/RWME	- 1 Copy
AFRL/RWMF	- 1 Copy
AFRL/RWMW	- 1 Copy
AFRL/RWMI	- 1 Copy